



Published in final edited form as:

Nat Chem Biol. 2019 August ; 15(8): 838–845. doi:10.1038/s41589-019-0321-7.

An excreted small-molecule promotes *C. elegans* reproductive development and aging

Andreas H. Ludewig^{1,*}, Alexander B. Artyukhin¹, Erin Z. Aprison², Pedro R. Rodrigues¹, Dania C. Pulido¹, Russell N. Burkhardt¹, Oishika Panda¹, Ying K. Zhang¹, Pooja Gudibanda¹, Ilya Ruvinsky^{2,*}, Frank C. Schroeder^{1,*}

¹Boyce Thompson Institute and Department of Chemistry and Chemical Biology, Cornell University, Ithaca, NY, USA

²Department of Molecular Biosciences, Northwestern University, Evanston, IL, USA

Abstract

Excreted small-molecule signals can bias developmental trajectories and physiology in diverse animal species. However, the chemical identity of these signals remains largely obscure. Here we report identification of an unusual *N*-acylated glutamine derivative, nacq#1, that accelerates reproductive development and shortens lifespan in *C. elegans*. Produced predominantly by *C. elegans* males, nacq#1 hastens onset of sexual maturity in hermaphrodites by promoting exit from the larval dauer diapause and by accelerating late larval development. Even at picomolar concentrations, nacq#1 shortens hermaphrodite lifespan, suggesting a trade-off between reproductive investment and longevity. Acceleration of development by nacq#1 requires chemosensation and depends on three homologs of vertebrate steroid hormone receptors. Unlike ascaroside pheromones, which are restricted to nematodes, fatty acylated amino acid derivatives similar to nacq#1 have been reported from humans and invertebrates, suggesting that related compounds may serve signaling functions throughout Metazoa.

Inter-organismal small molecule signaling has been implicated in regulating multiple aspects of animal biology¹. In addition to shaping behaviors on relatively short timescales, chemo-social signals can also modulate gene expression programs that regulate development and physiology. Such longer-lasting changes often occur in response to chemical messages from particularly salient emitters, such as potential mates and competitors. For example,

Users may view, print, copy, and download text and data-mine the content in such documents, for the purposes of academic research, subject always to the full Conditions of use:http://www.nature.com/authors/editorial_policies/license.html#terms

*Corresponding authors Ilya Ruvinsky; ilya.ruvinsky@northwestern.edu, Frank Schroeder, fs31@cornell.edu.

Author Contributions

I.R. and F.C.S. supervised the study. A.H.L., A.B.A., I.R., and F.C.S. designed experiments. A.H.L., A.B.A., E.Z.A., P.R.R., D.C.P., R.N.B., P.G., and O.P. performed chemical and biological experiments R.N.B. and Y.K.Z. performed syntheses. I.R. and F.C.S. wrote the paper with input from other authors.

Online Content

Methods, along with any additional Supplementary Data display items and source data, are available in the online version of the paper; references unique to these sections appear only in the online paper.

Supplementary Information is available in the online version of the paper.

Competing financial interests

The authors declare no competing financial interests.

Drosophila melanogaster males exposed to female sex pheromones showed complex physiological changes consistent with expectation of mating². In mice, sexually mature males produce a small-molecule signal that induces earlier onset of the first estrus in peripubescent females³.

Previous studies in *C. elegans* demonstrated that individuals of both sexes excrete yet unidentified signals that alter development: *C. elegans* hermaphrodites develop faster on hermaphrodite-conditioned plates⁴ or following exposure to trace quantities of male-excreted metabolites⁵ (Fig. 1a). Accelerated progression through larval development in response to small-molecule signals from other individuals in a population appears as a direct opposite of larval arrest of development at the dauer stage, which is triggered by harsh environmental conditions in combination with excreted pheromones called ascarosides⁶⁻⁸. The ability to modify the rate of development in response to environmental conditions may be particularly important to short-lived animals in ephemeral boom-and-bust habitats⁹. Notably, the ability to accelerate development in response to male and hermaphrodite signal appears to come at a cost – both of these treatments reduce hermaphrodite lifespan (Fig. 1a)^{4,10-12}, mirroring the effect of female sex pheromones on longevity of *Drosophila* males³.

Similar effects of chemical signals on developmental time and longevity observed in divergent species raises the possibility that at least some of the underlying mechanisms are conserved among Metazoa. However, little is known regarding the chemical nature of the signal(s) and the regulatory pathways that implement their effects. In this study we identified an excreted small-molecule, nacq#1 (**1**), that promotes sexual maturation of *C. elegans* hermaphrodites by modulating conserved signaling pathways. nacq#1 is an *N*-acylated glutamine that belongs to a class of small-molecules found in diverse animal lineages, unlike the previously described ascarosides, which appear to be largely restricted to nematodes. Further, we demonstrate that the effects of nacq#1 are mediated by the chemosensory system and a network of nuclear hormone receptors. Our findings expand the universe of known metabolites that specifically alter development and physiology in members of the same species. Because nacq#1 is predominantly present in male excretions, our results contribute to a better understanding of sexual dimorphism of metabolism, particularly with respect to excreted signaling compounds. Finally, the availability of a pure molecule that potently alters development and lifespan, offers a new tool for the study of mechanisms that regulate development and longevity in response to social signals.

Results

Excreted metabolites accelerate development and aging

In pursuit of the specific molecule(s) that accelerate *C. elegans* development and aging, we first compared the properties of the male- and hermaphrodite-excreted activities. Analyses of hermaphrodite development on plates conditioned by *exo*-metabolomes (Fig. 1b) revealed that male excretions were ~10-fold more potent than those of hermaphrodites. Accordingly, *exo*-metabolomes from *him-5* cultures, which contain >30% males, were more potent at accelerating sexual maturation than extracts of wildtype cultures, which are >99% hermaphrodite (Fig. 1c). *daf-22* males, which are defective in peroxisomal β -oxidation ($p\beta O$), accelerate hermaphrodite development as well as wildtype males⁵, indicating that the

active compound(s) is likely not an ascaroside pheromone, which are p β O-dependent^{13,14}. Similarly, the hermaphrodite-excreted activity is *daf-22*-independent (Supplementary Fig. 1 and ref.⁴). These results suggested that developmental acceleration and lifespan shortening are likely caused by a metabolite(s) that is excreted in higher quantities by males than hermaphrodites and does not belong to known families of *C. elegans* pheromones.

Identifying *nacq#1* via comparative metabolomics

To determine the chemical identity of the acceleration signal, we pursued a two-pronged approach, combining comparative metabolomics with activity-guided fractionation. To identify metabolites that are excreted in greater amounts by males, we compared *exo*-metabolomes from wildtype cultures and *him-5* cultures (Fig. 2a). High-resolution HPLC-MS using the XCMS platform^{15,16} revealed more than 20 compounds that were at least 3-fold enriched in *him-5* cultures relative to wildtype and thus represented plausible candidates for the acceleration signal (Supplementary Table 1). We then fractionated the *him-5* metabolome, using the onset of egg laying to measure developmental acceleration (Supplementary Fig. 2)⁴. For this assay we used *daf-22* worms, because this mutant does not produce ascaroside pheromones¹³, which may antagonize the activity of the acceleration signal⁴. The activity-guided fractionation revealed three active fractions, which were analyzed for the presence of metabolites enriched in *him-5* cultures. The two most abundant *him-5*-enriched compounds were detected in the most robustly active fraction, F13, but not in adjacent inactive fractions, F12 and F14 (Fig. 2b), and thus were selected as most likely candidates for the acceleration signal. Tandem MS analysis suggested that these compounds represent two isomeric fatty acylated amino acid derivatives that do not correspond to any previously reported metabolites (Fig. 2b, Supplementary Fig. 3). Following isolation of the compounds via preparative HPLC, we determined their structures via NMR spectroscopic analysis, which revealed *cis* and *trans* isomers of a triply unsaturated 10 carbon fatty acid attached to the amino acid glutamine. The absolute configuration of the glutamine moiety was determined using Marfey's reagent (Supplementary Fig. 4). We named the *cis* and *trans* isomers *nacq#1* (*N*-acyl glutamine#1) and *nacq#2* (**2**), respectively (Fig. 2b). *nacq#1* isomerizes into *nacq#2* under physiological conditions, suggesting that *nacq#1* is the primary biosynthetic product.

HPLC-MS analysis of *endo*- (worm body extracts) and *exo*-metabolomes showed that *nacq#1* production commences around the time of larval-to-young adult transition, approximately corresponding to sexual maturity, and declines shortly thereafter (Fig. 2c, Supplementary Figs. 5a,b). Moreover, similar to the dauer pheromone, e.g. *ascr#3* (**3**), *nacq#1* is primarily found in the *exo*-metabolome, as would be expected for an interorganismal signaling molecule (Supplementary Fig. 5a). In line with the estimate from functional assays of total *exo*-metabolomes (Fig. 1b), we found that males excrete ~10-fold more *nacq#1* than hermaphrodites (Fig. 2d), and that this compound is about three-fold more abundant in male-enriched *him-5* mutant cultures (>30% male) than in wildtype cultures (Supplementary Fig. 5c).

Given that *nacq#1* incorporates a (ω -3) polyunsaturated fatty acid, we asked whether its biosynthesis requires the fatty acid desaturases *fat-2* and *fat-1*, which are required for the

introduction of (ω -6) and (ω -3) double bonds in *C. elegans*, respectively, e.g. in the conversion of oleic acid (**4**) to linoleic acid (**5**) and α -linolenic acid (**6**) (Fig. 2e). nacq#1 production was largely abolished in *fat-1* and *fat-2* mutant worms (Fig. 2f), indicating that nacq#1 biosynthesis proceeds via longer-chained polyunsaturated fatty acids. Further, consistent with the observation that developmental acceleration by male- and hermaphrodite-derived *exo*-metabolomes is not dependent on the ascaroside biosynthetic enzyme *daf-22* (Supplementary Fig. 1 and ref.^{4,5}), nacq#1 biosynthesis is not affected by loss of *daf-22* in wildtype (Fig. 2f) or *him-5* mutant background (Supplementary Fig. 5c). We confirmed that biosynthesis of ascaroside pheromones, e.g. the dauer pheromone component ascr#3, is abolished in the *daf-22* mutants (Figs. 2f). Further, we found that nacq#1 biosynthesis is not strongly affected by nutritional conditions (Supplementary Fig. 6).

nacq#1 accelerates development and shortens lifespan

To explore the biological properties of nacq#1, we developed a short synthesis that provided access to pure nacq#1 and related compounds (Fig. 3a). The triply unsaturated fatty acid chain in nacq#1 was derived from (3*Z*)-hexenol (**7**) and aldehyde **8**, which after conversion of **7** to phosphonium salt **9**, Wittig reaction, and hydrolysis yielded (2*E*,4*Z*,7*Z*)-decatrienoic acid (**10**). Acid **10** was then coupled to L-glutamine *t*-butyl ester followed by acidic deprotection to furnish synthetic nacq#1 that was used for all subsequent biological experiments. First, we confirmed that synthetic nacq#1 at pico- to low nanomolar concentrations accelerated reproductive development, by measuring the onset of egg laying (Fig. 3b, Supplementary Fig. 7a) and the age of attainment of adult morphology (Fig. 3c, Supplementary Figs. 7b, c). Higher concentrations of nacq#1 are less effective, resulting in a bell-shaped dose response curve, as is the case for responses to other small molecule signals in *C. elegans*^{17,18} and other species¹⁹. Hermaphrodites produce on the order of 16 femtomoles/individual of nacq#1 during the L4-to-young adult transition, corresponding to accumulation of picomolar concentrations of nacq#1 on conditioned plates (Fig. 2c), consistent with the range of active concentrations observed for synthetic nacq#1. In contrast, neither nacq#2 nor the free fatty acid (nacq#1 without glutamine) were active at any of the tested concentrations (Supplementary Fig. 8). Similarly, the most abundant male-enriched ascaroside, ascr#10 (**11**),²⁰ did not alone accelerate larval development in hermaphrodites, nor did it synergize with nacq#1 (Supplementary Fig. 9). Male-excreted compounds shorten the last larval stage (L4)⁵, and we found that synthetic nacq#1 likewise specifically accelerates this stage of development (Fig. 3d). Given the relatively modest extent of acceleration – approximately 2–3 hours, or ~3–5% of the total egg-to-egg developmental time – we tested whether there was any impact on the onset of reproduction. Hermaphrodites raised in the presence of nacq#1 on average produced ~30% more offspring during the first day of egg laying (Fig. 3e), a notable advantage for a species with a fast boom-and-bust life cycle²¹.

Next, we asked whether nacq#1 could also explain the observation that the presence of males¹⁰⁻¹² and, under some conditions, high population density,⁴ shorten the lifespan of hermaphrodites. Previous studies had shown that the lifespan-shortening effect of male *exo*-metabolome is at least partly dependent on the ascaroside biosynthetic enzyme *daf-22*^{11,12},

implicating as one factor the ascaroside *ascr#10*, which is excreted by males much more abundantly than hermaphrodites²⁰. To test whether *nacq#1* affects hermaphrodite lifespan, we used a single-worm assay that largely prevented the potentially confounding exposure of test animals to excreted metabolites from other worms. We found that exposure to picomolar concentrations of *nacq#1* significantly reduced lifespan from 16.3 days to 13.6 days (Fig. 3f), similar to lifespan shortening observed for hermaphrodites exposed to male *exo*-metabolome¹¹. In contrast, *nacq#1* had little effect in lifespan assays conducted at higher population density.

Because males produce *nacq#1* much more abundantly than hermaphrodites (Fig. 2d), our results suggest that individual males and hermaphrodites at high population density produce sufficient quantities of *nacq#1* (and possibly additional substances) to shorten hermaphrodite lifespan. However, singled hermaphrodites and groups of hermaphrodites have similar lifespan in aging assays set up as young adults⁴ or L4 larvae^{12,22}. Combined with our finding that *nacq#1* is excreted primarily during the transition from the L4 larval stage to young adults (Fig. 2c), these results indicate that lifespan is determined not only by population density during adulthood, but also by the social conditions, and associated exposure to *nacq#1* and other pheromones, experienced by larvae between hatching and the onset of adulthood.

Next we assessed the effects of *nacq#1* and *ascr#10*, both of which are produced in larger quantities by males, on hermaphrodite lifespan. We confirmed that *ascr#10* shortens hermaphrodite lifespan, and found that the lifespan-shortening effects of *ascr#10* and *nacq#1* are additive at low concentrations (Fig. 3g, Supplementary Fig. 10), and they may act via partly independent molecular mechanisms. Notably, *nacq#1* shortened hermaphrodite lifespan significantly at concentrations as low as 1 pM, similar to the lifespan-shortening effect of *ascr#10* at 4 nM. Since *nacq#1* is active at lower concentrations than *ascr#10*, and given that males excrete similar amounts of *ascr#10*²⁰ and *nacq#1*, the effect of *nacq#1* on hermaphrodite lifespan may outweigh that of *ascr#10* under natural conditions; however, ascarosides²³ are chemically much more stable than *nacq#1*, and the spatial and temporal deposition of these compounds by males may differ.

Antagonism of *nacq#1* and dauer inducing ascarosides

To gain insight into the mechanisms underlying the effects of *nacq#1* on *C. elegans* development and lifespan, we investigated interaction of *nacq#1* with a subset of ascaroside pheromones, known to divert development into the dauer diapause, including *ascr#2* (**12**) and *ascr#3* (Fig. 4a)^{17,24,25} and extend lifespan²⁶. Dauer larvae are adapted to long-term survival under adverse environmental conditions and have been used extensively as a model to study conserved mechanisms of developmental plasticity and aging²⁷⁻²⁹. When encountering conditions conducive to growth and reproduction, dauer larvae resume development into reproductive adults. Our results suggest that *nacq#1* and dauer-inducing ascarosides have generally opposing effects on reproductive development. First, *nacq#1* hastens the onset of reproduction (Fig. 3b), whereas ascaroside pheromones promote developmental arrest. Second, *nacq#1* and high population density (Fig 3b, Supplementary Fig. 1)⁴ accelerate development more strongly in ascaroside-deficient *daf-22* mutants than in

wildtype worms. Addition of dauer-inducing ascarosides reduced developmental acceleration by *nacq#1*, confirming that these ascarosides antagonize the effects of *nacq#1* (Fig. 4b).

Whereas ascarosides are abundantly produced by larvae and adult worms³⁰, *nacq#1* production is transient, peaking around sexual maturation (Fig. 2c), suggesting that it may serve as a signal of conditions that support reproductive development and promote exit from the dauer stage. To test this idea, we used *daf-2*/insulin receptor and *daf-7*/TGF- β mutants, which constitutively form dauers at non-permissive temperatures^{28,31}. *nacq#1* promoted dauer exit in *daf-7(m62)* and *daf-2(e1368)* mutants (Figs. 4c,d) and also counteracted the suppression of dauer exit by ascarosides in wildtype animals (Fig. 4e). In contrast, *nacq#1* did not significantly affect ascaroside-triggered dauer entry (Supplementary Fig. 11), indicating that it primarily serves as a “dauer-exit” pheromone. These results show that *nacq#1* and ascarosides exert mutually opposing effects on development.

***nacq#1* requires NHR-dependent and chemosensory pathways**

Ascarosides trigger dauer development primarily via downregulation of insulin- and TGF- β signaling, which abolishes the biosynthesis of steroidal ligands of DAF-12, a homolog of mammalian steroid hormone receptors³¹⁻³³. The unliganded DAF-12 then binds to its co-repressor DIN-1/SHARP, causing developmental arrest at the dauer stage³⁴. We asked whether acceleration of development by *nacq#1* depends on insulin- and TGF- β signaling and tested mutants of the FOXO-transcription factor *daf-16*, the target of the *daf-2* receptor, and a TGF- β ligand, *daf-7*. We found that developmental acceleration was abolished in both *daf-16* mutant alleles, whereas *daf-7* mutants behaved similar to wildtype (N2) (Fig. 5a). Next, we tested mutants of DAF-12 and its two paralogs, NHR-8 and NHR-48. Whereas NHR-8 has been shown to regulate steroid hormone biosynthesis and thus link steroid hormone signaling and lifespan^{35,36}, little is known about the role of NHR-48 for development. We found that developmental acceleration by *nacq#1* was abolished in null mutants of all three NHRs (Fig. 5b, Supplementary Figs. 12a,b). To remove possible confounding interference from ascaroside pheromones, we also tested double mutant combinations between *daf-22* and *nhr-8*, *nhr-48*, and *daf-12*, which confirmed that these NHRs are required for developmental acceleration by *nacq#1* (Supplementary Fig. 12a). Consistent with a model in which *nacq#1* engages conserved development pathways, we detected this compound (and *nacq#2*) in *C. briggsae* (Fig. 5c) and other *C. elegans* relatives (Supplementary Fig. 13).

As an interorganismal signaling molecule, *nacq#1* could serve as a ligand for one of the required NHRs or, alternatively, could be perceived via chemosensation. Chemosensory neurons regulate dauer^{37,38} and lifespan^{39,40}, and have been implicated in the lifespan-shortening effects of male excretions¹¹. Whereas cell culture luciferase assays showed no evidence for activation of NHR-8 and NHR-48 by *nacq#1* (Supplementary Fig. 14), developmental acceleration by *nacq#1* was abolished or strongly reduced in *osm-6* and *che-13* mutants, which are defective in processing of chemosensory signals (Fig. 5b, Supplementary Figs. 12c,d). In addition, developmental acceleration by *nacq#1* is abolished (ASI) or reduced (ASK, ASJ) in worms lacking chemosensory neurons implicated in dauer

regulation^{38,41} (Fig. 5d). Although the exact mechanism of *nacq#1* perception remains to be elucidated, our results indicate that *nacq#1* is perceived via chemosensory circuits that trigger downstream signaling pathways targeting conserved steroid hormone receptors.

Discussion

Males and, to a lesser extent, hermaphrodites excrete a small molecule signal, *nacq#1*, that antagonizes diapause and accelerates development, hastening sexual maturation, but at the expense of a reduced lifespan (Fig. 5e). Because of the associated costs, reproductive commitment may be singularly attuned to signals from potential mates and competitors. In natural habitats, *C. elegans* is often found as developmentally arrested, dispersing dauer larvae⁹. A small molecule excreted upon reaching sexual maturity, *nacq#1* may indicate that sufficient resources are available to exit dauer and resume reproductive development. *nacq#1* further accelerates sexual maturation in larvae that are already developing into adults. This latter role of *nacq#1*, predominantly produced by males, is reminiscent of the signal produced by sexually mature male mice that induces earlier onset of the first estrus in peripubescent females³. These parallels suggest that signals excreted primarily by males modulate similar developmental processes in divergent animal lineages.

Downstream of chemosensation, *nacq#1* regulates development via transcription factors of the NR1 subfamily⁴², which includes steroid hormone receptors such as the vitamin-D receptor and liver-X receptor that coordinate vertebrate development⁴³. Our results suggest that the antagonism between *nacq#1* and dauer-inducing ascarosides may result from differential regulation of the three NR1 family members in *C. elegans*, since the effects of these ascarosides on development primarily depend on DAF-12, whereas acceleration of development by *nacq#1* also strictly requires NHR-8 and NHR-48 (Fig. 5b, Supplementary Figs. 12a,b). Correspondingly, dauer-inducing ascarosides and the dauer-exit promoting *nacq#1* have opposing effects on lifespan: whereas these ascarosides extend lifespan²⁶, *nacq#1* reduces longevity (Fig. 3f), consistent with a trade-off between reproductive investment and somatic maintenance^{44,45}. Two additional points deserve to be mentioned. First, whereas some ascarosides extend lifespan, others such as *ascr#10*, shorten it, likely via mechanisms that are at least somewhat independent from those that mediate activity of *nacq#1*. Second, although the *nacq#1*-induced shortening of the last larval stage by 2–3 hours could represent the beginning of a faster rate of aging that ultimately leads to a shortened lifespan, these two processes may also be mechanistically decoupled. Overall, our findings present a picture of a pull-push system of small-molecule signals that fine-tune development and longevity in response to changing social environments by modulating conserved gene regulatory networks (Fig. 5e).

The chemical structure of *nacq#1* suggests parsimonious use of simple building blocks from primary metabolism – the amino acid glutamine and an unusual, triply unsaturated ten-carbon fatty acid that could be derived from canonical ω -3 fatty acids, e.g. eicosapentaenoic or linolenic acid. Notably, unusual fatty acylated glutamines have been reported from multiple animal phyla. For example, acylated glutamines, e.g. **(13)**, that feature an uncommon branched heptanoyl moiety occur in human sweat⁴⁶ (Fig. 5f). It is unclear whether these human metabolites serve a biological function, as may be suggested by the

otherwise uncommon fatty acid moieties. In addition, amino acid derivatives of long-chain fatty acids have been implicated in intra-and inter-organismal signaling in vertebrates^{47,48} and invertebrates^{49,50}, e.g. volicitin (**14**). Our discovery of *nacq#1* as a regulator of development and lifespan in *C. elegans* suggests that related small molecules may serve signaling functions throughout Metazoa.

ONLINE METHODS

Nematode and bacterial strains.

Unless indicated otherwise, worms were maintained on Nematode Growth Medium (NGM) 6 cm diameter Petri dish plates with *E. coli* OP50 (<http://www.wormbook.org/methods>)⁵¹. The following *C. elegans* strains were used: Wild type Bristol N2, FCS1 *daf-22(ok693)*, DR476 *daf-22(m130)*, AA86 *daf-12(rh61 rh411)*, PR811 *osm-6(p811)*, SP1734 *osm-6(m511)*, CB3323 *che-13(e1805)*, AE501 *nhr-8(ok186)*, *nhr-8(ok186);daf-12(rh61 rh411)*, AA107 *nhr-48(ok178)*, DR466 *him-5(e1490)*, CB467 *him-5(e1467)*, CF1038 *daf-16(mu86)*, GR1352 *daf-16(mgDf47)*, GR1395 *mgIs49 [mlt-10::GFP-pest;ttx-1::GFP]*, DR62 *daf-7(m62)* and DR1572 *daf-2(e1368)*, RB1795 *fat-1(ok2323)*, BX26 *fat-2(wa17)*, ASI(-) PY7505 *oyIs84[Pgpa-4::ced-3(p17), Pgcy-27::ced-3(p15), Pgcy-27::gfp, Punc-122::dsRed]*, ASK(-) PS6025 *qrIs2[sra-9::mCasp1]*, ASJ(-) ZD762, *mgIs40[daf-28p::nls-GFP]; jxEx100[trx-1::ICE + ofm-1::gfp]*, FCS23 [*nhr-48(ok178); daf-22(ok693)*], FCS24 [*nhr-8(ok186); daf-22(ok693)*], and FCS30 [*daf-12(rh61, rh411); daf-22(ok693)*] were generated by crossing FCS1 *daf-22(ok693)* males with AE501 *nhr-8(ok186)*, AA107 *nhr-48(ok178)* or AA86 *daf-12(rh61, rh411)* hermaphrodites, respectively. Genotypes were confirmed using PCR. In addition, we used AF16 *C. briggsae*, NKZ2 *C. inopinata*, and CB5161 *C. brenneri*.

Time-of-development assays based on morphological criteria⁵.

Two different protocols were used to measure time of development based on morphological criteria. In the first experimental set-up (shown in Fig. 1b, Supplementary Figs. 5b, 7b, 12b, c), small populations of worms were tested. Synchronized cultures of L1 larvae were prepared by hypochlorite treatment of gravid hermaphrodites⁵². After treatment, the liberated eggs were allowed to hatch in M9 buffer overnight. The following morning, the resulting population of arrested L1 larvae was deposited onto the prepared (e.g. metabolome-conditioned, see below) plates at a density of 20–40 larvae per plate. After 48 hours at 20 °C, the plates were placed at 4 °C until examined under a dissecting scope.

In the second protocol (shown in Fig. 3c, Supplementary Figs. 7c, 9), L1 larvae were singled to either control or conditioned plates just after release from arrest as previously described⁵. These hermaphrodites were monitored every two hours starting at 49 hours after release from arrest until they had reached adulthood. The numbers of their progeny were counted 72 hours after release from L1 arrest (as shown in Fig. 3e). Developmental staging was based on vulval and gonadal morphology⁵³. All assays were repeated at least three times, unless noted otherwise. For source data, see Supplementary Dataset.

To condition plates with *exo*-metabolome preparations (Fig. 1b), mating plates of males and hermaphrodites were pooled and the resulting population was subjected to hypochlorite treatment to produce a synchronized mixed-gender culture. Separate age-matched populations of males and hermaphrodites were segregated at the L4 stage. The following day, worm *exo*-metabolome preparations were collected using a previously method²⁰ with some modification. One hundred worms, either males or hermaphrodites, were picked into 100 μ L of water in 200 μ L PCR tubes. Worms were incubated for 24 hours at 21 °C with shaking at 220 rpm. The liquid was filtered over sterile cotton to exclude the worms. *Exo*-metabolome was applied to NGM plates in 20 μ L drops including 5 μ L of OP50, overlaying and drying each drop until the desired amount of *exo*-metabolome was reached. Eggs or L1 larvae that were not filtered by the cotton were manually removed. Plates were refrigerated until use. For data shown in Fig. 1b, see Supplementary Dataset.

To condition plates with live animals, a 2-hour timed egg lay was done with mated hermaphrodites. “L3 plates” were conditioned by 10 worms that were between the ages of 38 to 47 hours post egg lay (just prior to the L2/L3 molt until just prior to the L3/L4 molt). When the larvae were added to the plates it was not easy to determine their sex. Therefore, the larvae were kept after removal from the plates and their sex was determined. Every plate had at least 4 out of 10 larvae that eventually developed into males. “L4 plates” were conditioned by 10 worms that were between the ages of 48 to 58 hours post egg lay (just after the L3/L4 molt and just prior to the L4/Adult molt). At this stage of development, it was possible to determine the sex of the larvae and each plate was conditioned with 5 L4 males and 5 L4 hermaphrodites. For data shown in Supplementary Fig. 5b, see Supplementary Dataset.

To condition with *nacq#1*, *nacq#1* was added to enough OP50 overnight culture to equal 20 μ L and spotted on the plate to achieve the indicated concentrations. For data shown in Fig. 3c, Supplementary Figs. 7b, 12b,c, see Supplementary Dataset. To condition with *ascr#10*, 2.2 pg of *ascr#10* (the amount known to induce behavioral and germline effects) was spread evenly over the surface of the agar plate with glass rod. The plates were kept at 20 °C overnight to allow the ascarioside solution to absorb into the agar and seeded with a 5 μ L spot of a 1:10 dilution of OP50 overnight culture.

Generation of *mlt-10* molting curves.

The data for the molting curves was generated using the protocol described previously⁵⁴ and relied on monitoring the level of GFP in *mlt-10::GFP* animals⁵⁵. Two experiments were started 12 hours apart, allowing observations of GFP expression throughout the four larval stages. In each experiment, a population of *mlt-10::GFP* animals was synchronized by hypochlorite bleaching as described above. Approximately 30 L1 larvae from this population were transferred to either control plates seeded with 20 μ L OP50 or treatment plates, which were seeded with 20 μ L OP50 containing 3 pg of *nacq#1*. Each of the two experiments consisted of 3 control (~90 animals) and 3 treatment (~90 animals) plates. Animals were examined every hour and scored for GFP fluorescence on a Leica MZ16F stereomicroscope. For data shown in Fig. 3d, see Supplementary Dataset 1.

Developmental acceleration assays with exo-metabolome samples and activity-guided fractionation.

Developmental acceleration assays, measuring the time point of first egg lay⁴, were performed using *daf-22(ok693)* hermaphrodites. Exo-metabolome samples from N2, *him-5(e1490)*, and *him-5(e1467)* worms, prepared as described¹³, were assayed undiluted or diluted 1:10, 1:100 and 1:1000 in 100% methanol. 100 μ L of fraction or dilution or pure methanol (as control) were then spread on 3.5 cm NGM plates, dried for 30 min, seeded with 35 μ L OP50 *E.coli* bacteria and incubated at 20 °C overnight. These plates were then used in acceleration assays, measuring the time point of first egg laying, as described above. Developmental acceleration (in hours) was calculated as the time difference between the time of first egg lay on untreated ISO plates minus time of first egg lay on conditioned ISO (or HD) plates. Assays were repeated at least 3 times, with 10–15 ISO plates used for assaying each metabolome sample.

To identify compounds that accelerate development, *him-5(e1490)* exo-metabolome samples were fractionated on preparative reverse-phase HPLC using an Agilent Zorbax Eclipse XDB-C8 column (9.4 \times 250 mm, 5 μ m particle diameter) and 0.1% aqueous formic acid-acetonitrile solvent gradient at a flow rate of 3.6 ml/min. Fractions were evaporated to dryness *in vacuo* and re-suspended in 2 ml of 2% ethanol/water solution. 100 μ L of each fraction (and 2% ethanol/water control) were spread on 3.5 cm plates, dried for 30 min, seeded with 35 μ L OP50 *E.coli* bacteria and incubated for 24 hours. Plates were used tested for acceleration of development of isolated (one worm per plate) *daf-22(ok693)* hermaphrodites, as described above. Assays were repeated three times, using 5–15 ISO plates for each fraction. For data shown in the Fig. 1c and Supplementary Fig. 2, see Supplementary Tables 2 and 4, respectively.

Time-of-development assays based on first egg lay⁴.

For synchronization, 50–100 worms (N2 or mutants, as specified) were allowed to lay eggs for 1 h on NGM plates seeded with OP50 *E. coli* bacteria, adult worms were removed and the resulting F1 generation was grown for 72 h at 20 °C. From those plates, 50–70 worms were transferred to a fresh 6 cm NGM plate (100 μ L fresh bacteria were spread onto the center of a plate and grown overnight at 23 °C to produce a bacterial lawn of approximately 2 cm diameter). Worms were allowed to lay eggs for 1–2 hours and either single eggs (for ISO plates) or 50–70 eggs (for High Density (HD) plates) - were transferred using a worm pick to fresh 3.5 cm plates containing 4 mL NGM agar, seeded with 35 μ L of freshly grown OP50 bacteria. The time point of egg transfer was defined as start time of the experiment. After 59 h at 20 °C, 10–20 worms from each condition (ISO and HD) were isolated by individual transfer onto fresh 3.5 cm NGM plates seeded with OP50 *E. coli* bacteria. Animals were scored for egg laying beginning at 60 h and then every hour. Animals were scored using a Leica DM 5500B microscope and a Q Imaging 200R camera. All assays were repeated at least three times, unless noted otherwise in the Supplementary Tables. For data shown in Supplementary Fig. 1, see Supplementary Table 3.

High resolution mass spectrometry.

Liquid chromatography was performed on a Dionex 3000 UPLC coupled with a Thermo Q-Exactive high-resolution mass spectrometer. HPLC separation was achieved using an Agilent Zorbax Eclipse XDB-C18 (2.1×150 mm 1.8 Micron particle size) maintained at 40 °C. Chromatographic conditions started with an isocratic gradient of 5% water with 0.1% formic acid and 95% acetonitrile until 1.5 min and then increasing linearly to achieve 100% acetonitrile at 13.5 min. *ascr#3*, *nacq#1* and *nacq#2* were quantified from data in ESI⁻ by integrating the peaks of their respective ion extracted chromatograms (< 2 ppm) at the previously standard verified retention times. Data are shown in Fig. 2b, Supplementary Fig. 3.

Determination of the absolute configuration of *nacq#1*.

Individual samples (100 µL) of 50 µM solutions of *nacq#1*, L-glutamine, and D-glutamine in methanol were evaporated in glass vials *in vacuo* and hydrolyzed with 200 µL of 6 N HCl at 90 °C overnight. The reaction was then evaporated *in vacuo* and the residue was dissolved in 100 µL of water. In addition, 50 µM stock solutions of the four amino acids L-Glu, D-Glu, L-Gln, and D-Gln were prepared in water. 100 µL of 1-fluoro-2,4-dinitrophenyl-5-L-alaninamide (L-FDAA, Marfey's reagent; 1% w/v in acetone) and 20 µL of 1 M NaHCO₃ were added to 50 µL of the hydrolyzed sample of *nacq#1* or the amino acid standards. After heating on a water bath at 37 °C for 1 h, reactions were quenched by adding 10 µL of 2 N HCl. The reactions of the *nacq#1* sample and amino acid standards were subjected to LC-MS analysis without further dilution (Micromass Quattro Ultima mass spectrometer coupled to Agilent 1100 HPLC; column: Agilent Zorbax Eclipse XDB-C18, 4.6 × 250 mm, 5 µm; injection 2 µL) using a linear gradient of water with 0.1% formic acid and acetonitrile (starting at 5% acetonitrile for 5 min, then ramping to 100% acetonitrile over 32 min; 1.0 ml/min flow rate; detection in the negative ionization mode). Analysis of Gln and Glu standards indicated that complete conversion of Gln to Glu took place during the acid hydrolysis step for both *nacq#1* and glutamine. Data is shown in the Supplementary Fig. 4.

Isolation and purification of *nacq#1* and *nacq#2*.

Medium from *C. elegans* mixed-stage culture (total volume 7 L, total number of worms ca. 3·10⁷) was lyophilized and extracted with methanol. Dried methanol extract was loaded onto Celite and fractionated on medium pressure reverse phase chromatography (86 g C18 Combiflash RediSep column). A 0.1% aqueous acetic acid-acetonitrile solvent gradient was used at a flow rate of 60 mL/min, starting with acetonitrile content of 0% for 10 min, which was increased to 100% over a period of 82 min. After assaying fractions by UPLC-MS, the relevant fractions were combined, solvent removed, and the residue was further fractionated on preparative reverse-phase HPLC using an Agilent Zorbax Eclipse XDB-C8 column (9.4 × 250 mm, 5 µm particle diameter) and 0.1% aqueous formic acid-acetonitrile solvent gradient at a flow rate of 3.6 ml/min. All fractions were assayed by LC-MS to confirm correct fractionation. Solvent from the fractions containing *nacq#1* and *nacq#2* was removed *in vacuo* and the residue was subjected to the second round of preparative HPLC on an ACE 5 C18-AR column (10 × 250 mm) using the same solvent gradient, which yielded a sample for NMR analysis (CD₃OD, Bruker AVANCE III HD, 800 MHz). Approximately 30 µg of each

nacq#1 and nacq#2 were isolated from 7 L of *C. elegans* medium. Chemical structures are shown in Fig. 2b.

Relative amounts of nacq#1 in *C. elegans* males and hermaphrodites.

Worms were picked into three 1.5 mL HPLC vials containing 100 μ L of M9 media each as follows: (a) 80 N2 L4 males, (b) 80 N2 L4 hermaphrodites, and (c) 40 N2 L4 males and 40 N2 L4 hermaphrodites. The vials were then incubated at 22 °C while shaking at 220 rpm. At 12 h and 24 h time points, the vials were centrifuged, and a 25 μ L aliquot of the supernatant media was removed and mixed with an equal volume of methanol to precipitate out proteins. This mixture was then centrifuged and 1 μ L of the supernatant was analyzed by LC-HRMS. Data are shown in Fig. 2d.

Quantification of ascr#3, nacq#1 and nacq#2 during development.

Worms were synchronized by treating gravid adults with alkaline hypochlorite solution and eggs were washed three times in M9. Eggs were then arrested in S-complete overnight to produce arrested L1s. Arrested L1 larvae were then seeded at a density of 4×10^5 animals per 300 mL of S-complete solution supplemented with concentrated OP50. Animals were then grown in liquid culture and collected at the following timings: 12 h for L1s, 24 h for L2s, 32 h for L3s, 40 h for mid-L4s and adults were collected at 58 h. Worms were visually inspected before collection to confirm the developmental stage. In a separate experiment, animals were grown to 43 h (mid-L4), 48 h, 53 h, 57 h and 61 h. Pellets and media were extracted as described, using 10 mL of methanol. Worms were separated from media by centrifugation and persistent OP50 was pelleted before collection of media for analysis. After lyophilization, worm pellets were homogenized in methanol using a glass homogenizer. Media and pellets were then extracted in 20 mL of pure methanol for 16 h with stirring. The methanol extract was then separated from insoluble materials by centrifugation, dried *in vacuo* and resuspended in 250 μ L of methanol for LC-MS analysis. Note that in this experiment, secreted compounds accumulate in the *exo*-metabolome from the L1 stage up until the collection time point. Data are shown in the insert of Fig. 2c and Supplementary Fig. 5a.

Estimation of nacq#1 production by hermaphrodites.

To quantify the amount of nacq#1 produced by *C. elegans* hermaphrodites, we first generated serial dilutions of synthetic nacq#1 standard in *fat-1* mutant metabolome extract (to account for ion suppression effects) for analysis via LC-MS, using the conditions described above. From these data a standard curve was generated after integrating the peak representing the nacq#1 molecular ion (293.15068 in ESI-), which was used to calculate nacq#1 concentrations in the *exo*-metabolome samples obtained at 57 h and 61 h in the time-course experiment described above. This analysis indicated that one hermaphrodite produces about 16 fmol during development through 61 h. Correspondingly, nacq#1 concentrations on a 6 cm plate (assuming a volume of 10 mL) with 20 hermaphrodites would be expected to reach 32 pM during development. Data are shown in Fig. 2c.

Quantification *nacq#1* production during different time windows through adulthood.

Synchronized L1 N2 larvae (prepared as above) were seeded at a density of 1×10^6 animals per 33 mL of S-complete solution supplemented with concentrated OP50. Animals were then grown in liquid culture, settled, and 25 mL of media frozen after 38 h, corresponding to the L4 stage. The worms were then rinsed two times in M9, rinsed one time in S-complete, and growth was continued in S-complete medium supplemented with concentrated OP50. The process was repeated, and media collected after 52 h (at which time the worms were young adults), 72 h, 96 h, 120 h, and 144 h for adults. After 144 h worms were pelleted and rinsed two times in M9 and one time in MQ H₂O. After lyophilization, worm pellets were homogenized with a tissue grinder. Media and pellets were extracted in 13 mL of pure ethanol for 16 h with stirring. The ethanol extracts were separated from insoluble materials by centrifugation, dried *in vacuo* and resuspended in 80 μ L of ethanol for LC-MS analysis as above. Data are shown in Fig. 2c.

Quantification of linoleic acid, α -linolenic acid, *nacq#1* and *ascr#3* in fat mutants.

Synchronized L1 larvae (prepared as above) were seeded at a density of 1×10^6 animals per 33 mL of S-complete solution supplemented with concentrated OP50. Animals were then grown in liquid culture and gravid adults were collected after 60 h. Worms were visually inspected before collection to confirm the developmental stage. Worms were separated from media by centrifugation and persistent OP50 was pelleted before collection of media for analysis. After lyophilization, the media was extracted in 13 mL of pure ethanol for 16 h with stirring. The ethanol extract was separated from insoluble materials by centrifugation, dried *in vacuo* and resuspended in 160 μ L of ethanol for LC-MS analysis as above. Data are shown in Fig. 2f.

Quantification of *ascr#3*, *nacq#1* and *nacq#2* in different bacterial dilutions.

Worms were synchronized by treating gravid adults with alkaline hypochlorite solution and eggs were washed three times in M9 and allowed to arrest as L1s overnight in M9. Approximately 7000 animals/plate were then transferred to 10 cm NGM plates with 2.5 mL of OP50 previously diluted in S-basal medium to the indicated concentrations. Final colony forming units (cfu) were confirmed after the final dilutions were made. The animals were allowed to reach the gravid adult stage, collected by centrifugation, and washed with S-basal medium prior to extraction. After lyophilization, worm pellets were homogenized in methanol using a glass homogenizer. These were then extracted in 10 mL of methanol, and the extract was then separated from insoluble material by centrifugation, dried *in vacuo*, and resuspended in 100 μ L of methanol for LC-MS analysis as above. Data are shown in Supplementary Fig. 6.

Identification of *nacq#1* in *C. briggsae*, *C. brenneri*, and *C. inopinata*.

For preparation of *C. briggsae* male and hermaphrodite *exo*- and *endo*-metabolome samples, mating plates were subjected to hypochlorite treatment to obtain age-matched populations. At about 45 hours post release from L1, 200 (counts per trial) hermaphrodites and, separately, 200 males were picked onto sparse lawn plates (50 μ L of a 1:100 dilution of OP50 overnight spread with a glass rod to form a lawn). The plates were left at room

temperature until all of the L4s had molted into adults. Adults were washed off the plates with M9 buffer into 15 mL conical tubes. The tubes were incubated at room temperature with shaking at 220 rpm for 24 h. After 24 h, the contents of the tubes were pooled and placed in a clinical centrifuge. The tube was spun at 1,625 x g for one minute. The supernatant was drawn off, leaving a small pellet of worms in the original tube, and placed in a second conical tube. All tubes were immediately frozen in liquid nitrogen and stored at -80°C until testing. *C. brenneri* and *C. inopinata* *exo*-metabolome samples were prepared analogously from mixed populations and analyzed by HPLC-MS as described above. Data are shown in Fig. 5c and Supplementary Fig. 13.

Developmental acceleration assays with nacq#1, nacq#2, and (2E, 4Z,7Z)-deca-2,4,7-trienoic acid.

To test pure compounds, 3.5 cm NGM plates were prepared as follows: 30 µg of nacq#1 or nacq#2 were dissolved in 2 mL 100% ethanol, providing 50 µM stock solutions. Stock solutions were further diluted in water to give 40 nM, 4 nM and 40 pM solutions. Control solutions for mock treatment had corresponding amounts of ethanol added. 100 µL of compound solution or mock solution were distributed onto the surface of a 3.5 cm plate containing 4 mL of NGM agar (1:40 dilution), resulting in final plate concentrations of 1 nM, 100 pM and 1 pM, respectively. For the experiments shown in Fig. 4b, plates additionally contained the indicated concentrations of ascariosides. Plates were dried with open lids for 30 min and seeded with 35 µL freshly grown OP50 bacteria. Bacterial lawns were allowed to grow over night. Developmental acceleration was assessed by measuring the time point of first egg laying, as described above. Developmental acceleration (in hours) was calculated as the time difference between the time of first egg lay on untreated ISO plates minus time of first egg lay on conditioned ISO (or HD) plates. For data shown in Figs. 3b, 4b, and 5 see Supplementary Tables 5, 11, and 13-15; for data shown in Supplementary Figs. 7a, 8, and 12, see Supplementary Tables 10, 13, and 14.

Lifespan assays with nacq#1.

50–60 hermaphrodite N2 worms from synchronized plates were placed onto 6 cm NGM plates with fresh *E. coli* OP50 bacteria and allowed to lay eggs for 1 h. From these plates, eggs were transferred onto experimental plates containing nacq#1 (at a concentration of 1 nM, 100 pM, 10 pM, or 1 pM) and/or ascr#10 (at a concentration of 400 nM or 4 nM) at densities of 1 egg per plate, or, for some assays, 10 or 25 eggs per plate. Ascr#10 concentrations were chosen based on an initial screen of a wider concentration range (Supplementary Table 10). Starting on day 3, worms were transferred daily onto fresh experimental plates until cessation of egg laying (~ day 8) and every 3 days after that, until the experiment was completed. Animals were scored as dead if they failed to respond to a tap on the head and tail with a platinum wire. Worms with internal hatching, exploders or animals that crawled off the plate were excluded. For data shown in Figs. 3f,g, and Supplementary Fig. 10, see Supplementary Tables 6-9.

Dauer assays.

Eggs from DR62 *daf-7(m62)* or DR1572 *daf-2(e1368)* were obtained by picking adult hermaphrodites to a fresh NGM plate and allowing egg lay to occur for 2 hours. Dauers

were obtained by allowing the eggs to develop at 25 °C for 3 days. Dauers were then selected by 1% SDS treatment for 5 minutes and transferred to assay plates containing nacq#1. Survival was scored after treating the animals with 1% SDS for 5 minutes. For dauer assays with wildtype worms, dauer induction was achieved by placing synchronized eggs on NGM pates containing an ascarside blend of 2 μM equimolar amounts of ascr#2, ascr#3, ascr#5, and ascr#8 and allowing them to develop at 26 °C for 3 days. Prior to assay setup dauers were selected with SDS as described above. Worms were allowed to stay on assay plates for 2.5 hours and scored after SDS selection as live/dead. For data shown in Figs. 4c-e and Supplementary Fig. 11, see Supplementary Table 12.

Luciferase assay for nacq#1-mediated NHR activation.

To determine whether nacq#1 activates transcription by steroid hormone receptor homologs in *C. elegans*, N-terminal flag tagged chimeric expression constructs of NHR-8 and NHR-48, consisting of DAF-12 DBD¹⁻⁴⁹⁹ and the respective LBD (NHR-8⁹¹⁻⁵⁶⁰, NHR-48¹⁶³⁻⁸¹⁷) were created. HEK 293T cells were seeded at 0.8 X 10⁶ cells per well in 96-well plates and transfected (per well) with 30 ng flag-tagged NHR expression vector, 30 ng of flag-tagged DIN-1e, 30 ng of *mir-241p* driven luciferase reporter, and 5 ng β-galactosidase expression vector (used as transfection normalization control) using the calcium phosphate precipitate method. Ethanol (negative control) or ethanol solutions of compounds (nacq#1 or 7-DA) were added 8 h post transfection at a final concentration of 100 nM, and the luciferase and β-galactosidase activities were measured by a Synergy 2 BioTek luminometer with Gen5 1.11 software 16 h post compound addition. Data are represented as luciferase RLU, normalized to β-galactosidase activity. Data shown represents 4 replicates, error bars ± S.D., two-tailed paired Student's t test. Data shown in Supplementary Fig. 14.

Synthesis and NMR spectroscopic data of nacq#1 and nacq#2.

See Supplementary Note – Synthetic Procedures.

Statistics.

Different statistical tests were used to validate the data obtained from the different experiments. Two-tailed unpaired Student's t-tests was used for the data in Figs. 1c, 3b, 4, and 5 as well as Supplementary Figs. 1, 2, 7a, 8, 11, 12a, and 12d. Two-tailed paired Student's t test was used for data shown in Supplementary Fig. 14. Significance of differences in time of development (in the experimental paradigm shown in Fig. 1b and similar) was computed using the χ^2 test.

Data availability

The authors declare that the data supporting the findings of this study are available within the article and its supplementary information files.

Supplementary Material

Refer to Web version on PubMed Central for supplementary material.

Acknowledgements

This work was supported in part by National Institutes of Health grants R01GM113692 (to F.C.S.), R01GM088290 (to F.C.S.), T32GM008500 (to R.N.B.), R01GM126125 (to I.R.), and by National Science Foundation grants IOS-1708518 and IOS-1755244 (to I.R.). F.C.S. is a Faculty Scholar of the Howard Hughes Medical Institute. This work made use of the Cornell University NMR Facility, which is supported, in part, by the NSF through MRI award CHE-1531632. We thank Navid Movahed and David Kiemle for assistance with mass spectrometry and NMR spectroscopy and Rubin Smith and Gary Horvath for technical support.

References

1. von Reuss SH & Schroeder FC Combinatorial chemistry in nematodes: modular assembly of primary metabolism-derived building blocks. *Nat Prod Rep* 32, 994–1006, doi:10.1039/c5np00042d (2015). [PubMed: 26059053]
2. Gendron CM et al. *Drosophila* life span and physiology are modulated by sexual perception and reward. *Science* 343, 544–548, doi:10.1126/science.1243339 (2014). [PubMed: 24292624]
3. Vandenberg JG Male odor accelerates female sexual maturation in mice. *Endocrinology* 84, 658–660, doi:10.1210/endo-84-3-658 (1969). [PubMed: 5812988]
4. Ludewig AH et al. Larval crowding accelerates *C. elegans* development and reduces lifespan. *PLoS Genet* 13, e1006717, doi:10.1371/journal.pgen.1006717 (2017). [PubMed: 28394895]
5. Aprison EZ & Ruvinsky I Sexually Antagonistic Male Signals Manipulate Germline and Soma of *C. elegans* Hermaphrodites. *Curr Biol* 26, 2827–2833, doi:10.1016/j.cub.2016.08.024 (2016). [PubMed: 27618262]
6. Ludewig AH & Schroeder FC Ascaroside signaling in *C. elegans*. *WormBook*, 1–22, doi:10.1895/wormbook.1.155.1 (2013).
7. Schroeder FC Modular assembly of primary metabolic building blocks: a chemical language in *C. elegans*. *Chem Biol* 22, 7–16, doi:10.1016/j.chembiol.2014.10.012 (2015). [PubMed: 25484238]
8. Butcher RA Small-molecule pheromones and hormones controlling nematode development. *Nat Chem Biol* 13, 577–586, doi:10.1038/nchembio.2356 (2017). [PubMed: 28514418]
9. Frezal L & Felix MA *C. elegans* outside the Petri dish. *eLife* 4, doi:10.7554/eLife.05849 (2015).
10. Shi C & Murphy CT Mating induces shrinking and death in *Caenorhabditis* mothers. *Science* 343, 536–540, doi:10.1126/science.1242958 (2014). [PubMed: 24356112]
11. Maures TJ et al. Males shorten the life span of *C. elegans* hermaphrodites via secreted compounds. *Science* 343, 541–544, doi:10.1126/science.1244160 (2014). [PubMed: 24292626]
12. Shi C, Runnels AM & Murphy CT Mating and male pheromone kill *Caenorhabditis* males through distinct mechanisms. *eLife* 6, doi:10.7554/eLife.23493 (2017).
13. Artyukhin AB et al. Metabolomic “Dark Matter” Dependent on Peroxisomal beta-Oxidation in *Caenorhabditis elegans*. *J Am Chem Soc* 140, 2841–2852, doi:10.1021/jacs.7b11811 (2018). [PubMed: 29401383]
14. von Reuss SH et al. Comparative metabolomics reveals biogenesis of ascarosides, a modular library of small molecule signals in *C. elegans*. *J Am Chem Soc* 134, 1817–1824, doi:10.1021/ja210202y (2012). [PubMed: 22239548]
15. Forsberg EM et al. Data processing, multi-omic pathway mapping, and metabolite activity analysis using XCMS Online. *Nat Protoc* 13, 633–651, doi:10.1038/nprot.2017.151 (2018). [PubMed: 29494574]
16. Tautenhahn R, Bottcher C & Neumann S Highly sensitive feature detection for high resolution LC/MS. *BMC Bioinformatics* 9, 504, doi:10.1186/1471-2105-9-504 (2008). [PubMed: 19040729]
17. Pungaliya C et al. A shortcut to identifying small molecule signals that regulate behavior and development in *Caenorhabditis elegans*. *Proc Natl Acad Sci U S A* 106, 7708–7713, doi:10.1073/pnas.0811918106 (2009). [PubMed: 19346493]
18. Aprison EZ & Ruvinsky I Counteracting Ascarosides Act through Distinct Neurons to Determine the Sexual Identity of *C. elegans* Pheromones. *Curr Biol* 27, 2589–2599.e2583, doi:10.1016/j.cub.2017.07.034 (2017). [PubMed: 28844646]

19. He J et al. Distinct signals conveyed by pheromone concentrations to the mouse vomeronasal organ. *J Neurosci* 30, 7473–7483, doi:10.1523/jneurosci.0825-10.2010 (2010). [PubMed: 20519522]
20. Izrayelit Y et al. Targeted metabolomics reveals a male pheromone and sex-specific ascaroside biosynthesis in *Caenorhabditis elegans*. *ACS Chem Biol* 7, 1321–1325, doi:10.1021/cb300169c (2012). [PubMed: 22662967]
21. Schulenburg H & Felix MA The Natural Biotic Environment of *Caenorhabditis elegans*. *Genetics* 206, 55–86, doi:10.1534/genetics.116.195511 (2017). [PubMed: 28476862]
22. Gems D & Riddle DL Genetic, behavioral and environmental determinants of male longevity in *Caenorhabditis elegans*. *Genetics* 154, 1597–1610 (2000). [PubMed: 10747056]
23. Srinivasan J et al. A blend of small molecules regulates both mating and development in *Caenorhabditis elegans*. *Nature* 454, 1115–1118, doi:10.1038/nature07168 (2008). [PubMed: 18650807]
24. Butcher RA, Fujita M, Schroeder FC & Clardy J Small-molecule pheromones that control dauer development in *Caenorhabditis elegans*. *Nat Chem Biol* 3, 420–422, doi:10.1038/nchembio.2007.3 (2007). [PubMed: 17558398]
25. Jeong PY et al. Chemical structure and biological activity of the *Caenorhabditis elegans* dauer-inducing pheromone. *Nature* 433, 541–545 (2005). [PubMed: 15690045]
26. Ludewig AH et al. Pheromone sensing regulates *Caenorhabditis elegans* lifespan and stress resistance via the deacetylase SIR-2.1. *Proc Natl Acad Sci U S A* 110, 5522–5527, doi:10.1073/pnas.1214467110 (2013). [PubMed: 23509272]
27. Golden JW & Riddle DL A pheromone influences larval development in the nematode *Caenorhabditis elegans*. *Science* 218, 578–580 (1982). [PubMed: 6896933]
28. Hu PJ Dauer. *WormBook*, 1–19, doi:10.1895/wormbook.1.144.1 (2007).
29. Kenyon C The plasticity of aging: insights from long-lived mutants. *Cell* 120, 449–460, doi:10.1016/j.cell.2005.02.002 (2005). [PubMed: 15734678]
30. Kaplan F et al. Ascaroside expression in *Caenorhabditis elegans* is strongly dependent on diet and developmental stage. *PLoS ONE* 6, e17804, doi:10.1371/journal.pone.0017804 (2011). [PubMed: 21423575]
31. Fielenbach N & Antebi A C. elegans dauer formation and the molecular basis of plasticity. *Genes Dev* 22, 2149–2165, doi:10.1101/gad.1701508 (2008). [PubMed: 18708575]
32. Mangelsdorf DJ et al. The nuclear receptor superfamily: the second decade. *Cell* 83, 835–839 (1995). [PubMed: 8521507]
33. Antebi A, Yeh WH, Tait D, Hedgecock EM & Riddle DL daf-12 encodes a nuclear receptor that regulates the dauer diapause and developmental age in *C. elegans*. *Genes Dev* 14, 1512–1527 (2000). [PubMed: 10859169]
34. Ludewig AH et al. A novel nuclear receptor/coregulator complex controls *C. elegans* lipid metabolism, larval development, and aging. *Genes Dev* 18, 2120–2133 (2004). [PubMed: 15314028]
35. Magner DB et al. The NHR-8 nuclear receptor regulates cholesterol and bile acid homeostasis in *C. elegans*. *Cell Metab* 18, 212–224, doi:10.1016/j.cmet.2013.07.007 (2013). [PubMed: 23931753]
36. Thondamal M, Witting M, Schmitt-Kopplin P & Aguilaniu H Steroid hormone signalling links reproduction to lifespan in dietary-restricted *Caenorhabditis elegans*. *Nat Commun* 5, 4879, doi:10.1038/ncomms5879 (2014). [PubMed: 25209682]
37. Bargmann CI & Horvitz HR Control of Larval Development by Chemosensory Neurons in *Caenorhabditis-Elegans*. *Science* 251, 1243–1246 (1991). [PubMed: 2006412]
38. Schackwitz WS, Inoue T & Thomas JH Chemosensory neurons function in parallel to mediate a pheromone response in *C. elegans*. *Neuron* 17, 719–728 (1996). [PubMed: 8893028]
39. Alcedo J & Kenyon C Regulation of *C. elegans* longevity by specific gustatory and olfactory neurons. *Neuron* 41, 45–55 (2004). [PubMed: 14715134]
40. Apfeld J & Kenyon C Regulation of lifespan by sensory perception in *Caenorhabditis elegans*. *Nature* 402, 804–809, doi:10.1038/45544 (1999). [PubMed: 10617200]

41. Park D et al. Interaction of structure-specific and promiscuous G-protein-coupled receptors mediates small-molecule signaling in *Caenorhabditis elegans*. *Proc Natl Acad Sci U S A* 109, 9917–9922, 10.1073/pnas.1202216109 (2012). [PubMed: 22665789]
42. Maglich JM et al. Comparison of complete nuclear receptor sets from the human, *Caenorhabditis elegans* and *Drosophila* genomes. *Genome Biol* 2, Research0029 (2001). [PubMed: 11532213]
43. Wollam J & Antebi A Sterol regulation of metabolism, homeostasis, and development. *Annu Rev Biochem* 80, 885–916, doi:10.1146/annurev-biochem-081308-165917 (2011). [PubMed: 21495846]
44. Gems D & Partridge L Genetics of longevity in model organisms: debates and paradigm shifts. *Annu Rev Physiol* 75, 621–644, doi:10.1146/annurev-physiol-030212-183712 (2013). [PubMed: 23190075]
45. Maklakov AA & Immler S The Expensive Germline and the Evolution of Ageing. *Curr Biol* 26, R577–r586, doi:10.1016/j.cub.2016.04.012 (2016). [PubMed: 27404253]
46. Kuhn F & Natsch A Body odour of monozygotic human twins: a common pattern of odorant carboxylic acids released by a bacterial aminoacylase from axilla secretions contributing to an inherited body odour type. *J R Soc Interface* 6, 377–392, doi:10.1098/rsif.2008.0223 (2009). [PubMed: 18682364]
47. Long JZ et al. The Secreted Enzyme PM20D1 Regulates Lipidated Amino Acid Uncouplers of Mitochondria. *Cell* 166, 424–435, doi:10.1016/j.cell.2016.05.071 (2016). [PubMed: 27374330]
48. Long JZ et al. Ablation of PM20D1 reveals N-acyl amino acid control of metabolism and nociception. *Proc Natl Acad Sci U S A* 115, E6937–e6945, doi:10.1073/pnas.1803389115 (2018). [PubMed: 29967167]
49. Schmelz EA, Engelberth J, Alborn HT, Tumlinson JH & Teal PEA Phytohormone-based activity mapping of insect herbivore-produced elicitors. *Proceedings of the National Academy of Sciences* 106, 653–657, doi:10.1073/pnas.0811861106 (2009).
50. Weiss LC et al. Identification of *Chaoborus* kairomone chemicals that induce defences in *Daphnia*. *Nat Chem Biol* 14, 1133–1139, doi:10.1038/s41589-018-0164-7 (2018). [PubMed: 30429602]

Methods-only References

51. Brenner S The genetics of *Caenorhabditis elegans*. *Genetics* 77, 71–94 (1974). [PubMed: 4366476]
52. Sulston J & Hodgkin J *Methods*. (1988).
53. Seydoux G, Savage C & Greenwald I Isolation and characterization of mutations causing abnormal eversion of the vulva in *Caenorhabditis elegans*. *Dev Biol* 157, 423–436 (1993). [PubMed: 8500652]
54. MacNeil Lesley T., Watson E, Arda HE, Zhu Lihua J. & Walhout Albertha J. M. Diet-Induced Developmental Acceleration Independent of TOR and Insulin in *C. elegans*. *Cell* 153, 240–252, doi:10.1016/j.cell.2013.02.049 (2013). [PubMed: 23540701]
55. Frand AR, Russel S & Ruvkun G Functional genomic analysis of *C. elegans* molting. *PLoS Biol* 3, e312, doi:10.1371/journal.pbio.0030312 (2005). [PubMed: 16122351]

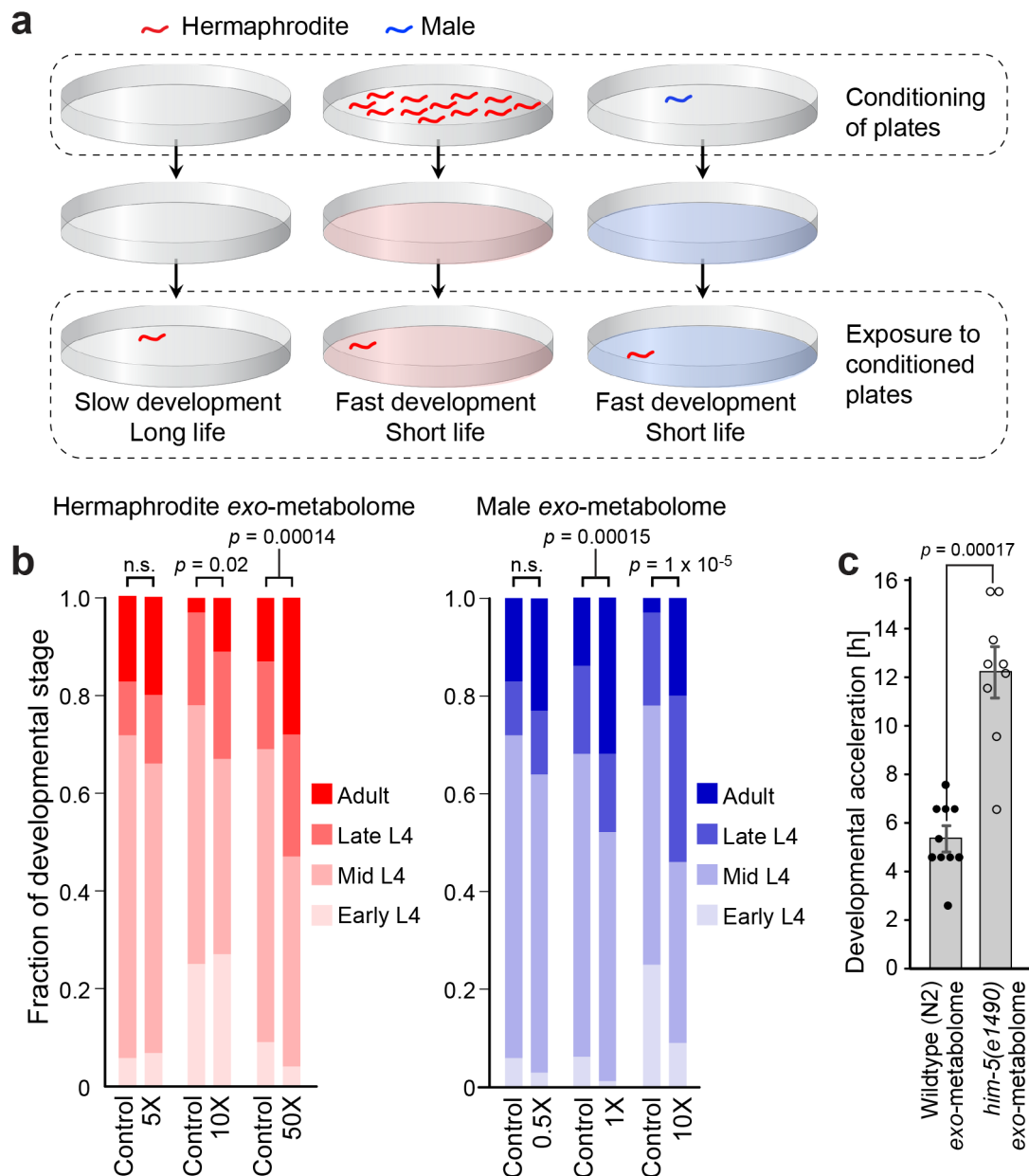


Figure 1. Excreted small molecules accelerate development in *C. elegans*.

a, Schematic of pre-conditioning experiment: worms on plates conditioned by single males or groups of hermaphrodites develop faster and have a shorter lifespan than worms raised on non-conditioned plates^{4,5,11}. **b**, Developmental progression of N2 hermaphrodites grown on plates conditioned with *exo*-metabolomes of N2 hermaphrodites or males ($n = 5$ biologically independent samples, where each replicate was one plate with ~ 30 animals, also see Supplementary Dataset). **c**, Developmental acceleration, measuring onset of egg lay, in *daf-22* hermaphrodites exposed to wildtype (N2, >99% hermaphrodites) and *him-5* ($\sim 30\%$ males) *exo*-metabolome ($n = 10$ worms for N2 and $n = 9$ worms for *him-5*). For data, see Supplementary Table 2. Error bars represent mean \pm s.e.m. and statistics were performed using the χ^2 test (Fig. 1b) or two-tailed *t*-test (Fig. 1c); n.s., not significant.

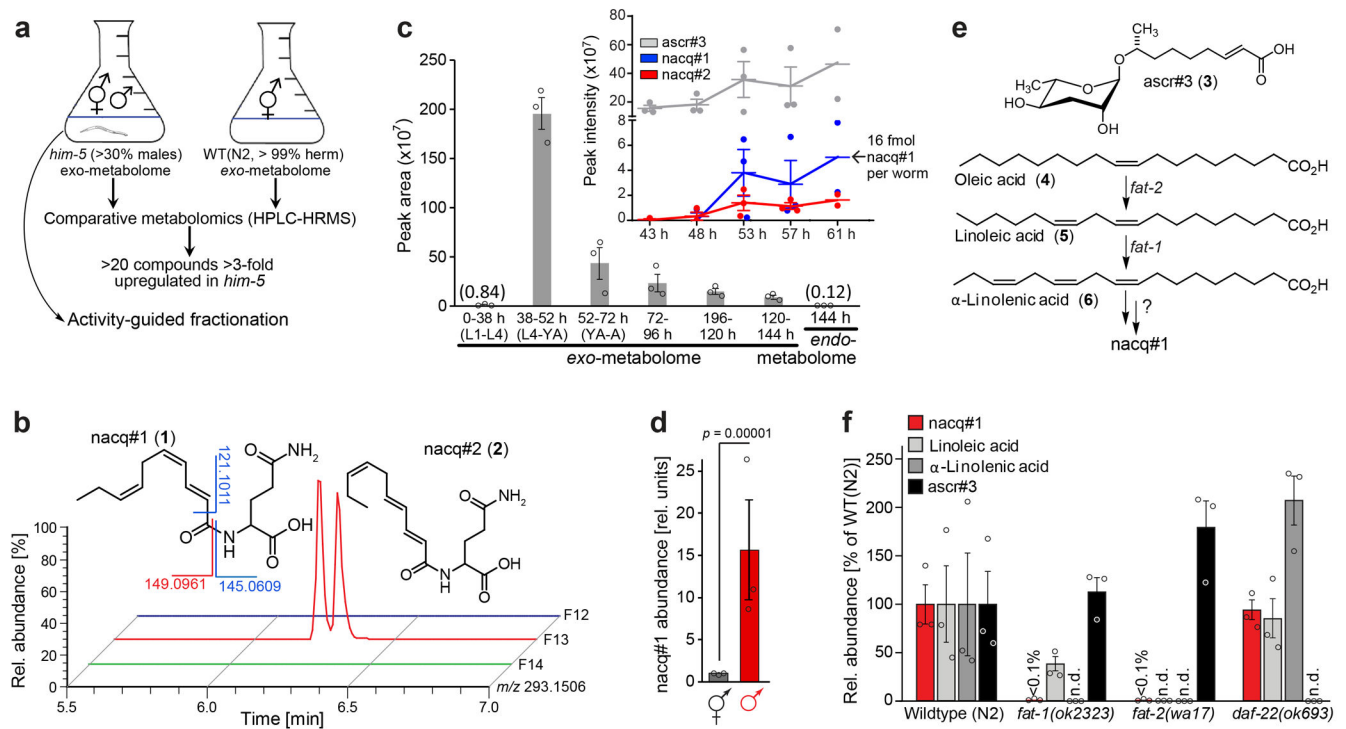


Figure 2 |. Identification of *nacq#1*, a signaling molecule primarily produced by males.

a, Experimental set up for comparative metabolomics with male-enriched *him-5* and wildtype N2 worm cultures. **b**, Ion chromatograms comparing HPLC fractions 12, 13 and 14 for *m/z* 293.1506 revealing presence of *nacq#1* and *nacq#2* in fraction 13 (this fractionation was performed once). **c**, HPLC-MS-based quantification of *nacq#1* in the *exo*-metabolomes collected during different time intervals, corresponding to different developmental stages. The insert shows data for cumulative excretion of *nacq#1*, *nacq#2*, and *ascr#3* up to specific time points during the L4-to-young adult transition. See Methods for details ($n = 3$ biologically independent samples per condition, except for the 61 h data point, $n = 2$). **d**, Relative amounts of *nacq#1* excreted by hermaphrodites and males ($n = 3$ biologically independent samples). **e**, Chemical structures of compounds in **f** and enzymatic roles of *fat-1* and *fat-2*. **f**, HPLC-MS-based quantification of *nacq#1*, linoleic acid, α -linolenic acid, and *ascr#3* in the *exo*-metabolomes of wildtype (N2), *fat-1(ok2323)*, *fat-2(wa17)*, and *daf-22(ok693)* worms ($n = 3$ biologically independent samples). Error bars represent mean \pm s.e.m.

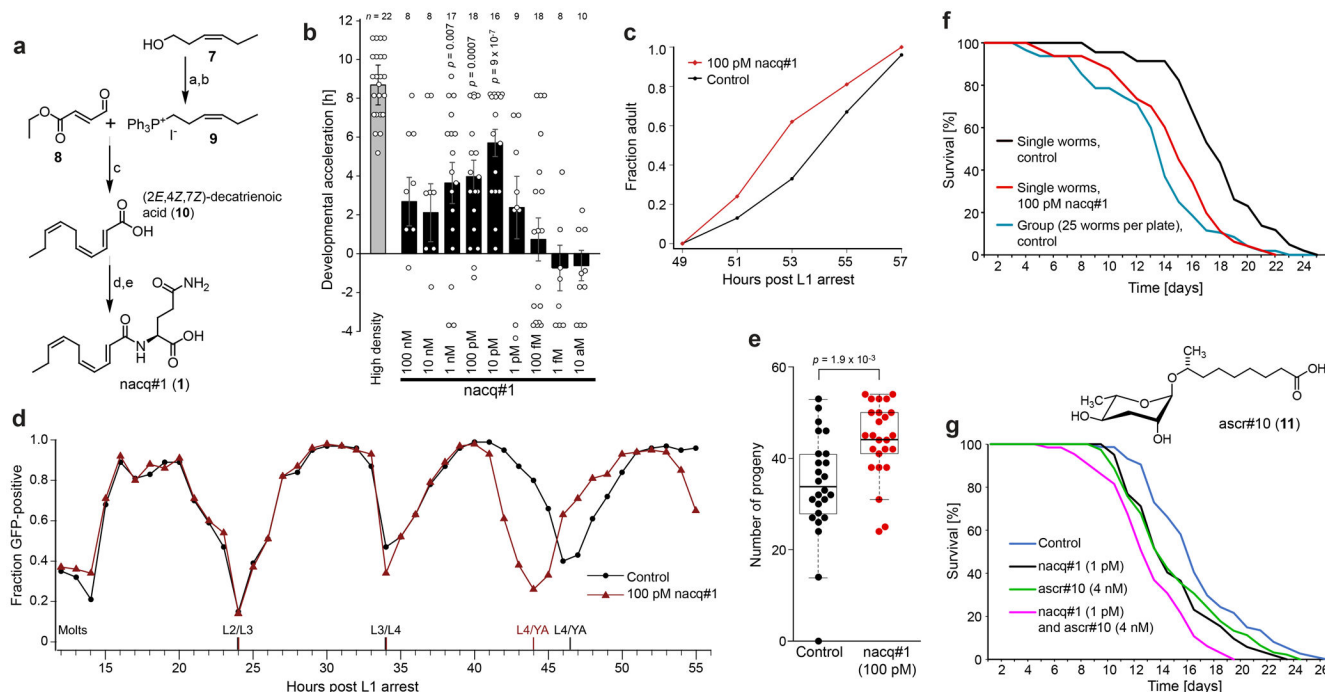


Figure 3 |. Biological properties of nacq#1.

a, Synthesis of nacq#1 and related molecules. **b**, Developmental acceleration assays measuring the onset of egg laying in *daf-22* worms exposed to nacq#1 (numbers of worms tested for each condition as indicated in Figure, also see Supplementary Table 5). **c**, Singled wild type hermaphrodites reach adulthood faster on plates conditioned with nacq#1 than animals on control plates ($n = 25$ (control) and $n = 21$ (nacq#1) worms per time point). Also see Supplementary Fig. 7c. **d**, Fractions of GFP-positive *mlt-10::GFP* animals developing on plates containing 100 pM nacq#1 compared to controls ($n = 99$ worms, 13-24 and 36-47 h (control), $n = 98$ worms, 25-35, 48-59 h (control), $n = 101$ worms, 13-24, 36-47 h (nacq#1 treated), $n = 95$ worms, 25-35, 48-59 h (nacq#1 treated)). Boundaries between larval stages are designated at GFP expression minima. **e**, Progeny production during the first day of reproduction. Each dot represents offspring of one parent ($n = 25$ hermaphrodite parents). **f**, Survival of groups of hermaphrodites (25 worms/plate, blue) and singled hermaphrodites (1 worm/plate) in the presence (red) or absence of nacq#1 (black). Assays were repeated 3 times for grouped worms and 6 times for singled worms. See Supplementary Table 6 for total number of worms. **g**, Survival of singled hermaphrodites on plates containing nacq#1, *ascr#10* or both compounds. Assays were repeated 5 times. Also see Supplementary Fig. 10 and Supplementary Tables 6-9. Error bars represent mean \pm s.e.m. and statistics were performed using two-tailed *t*-tests.

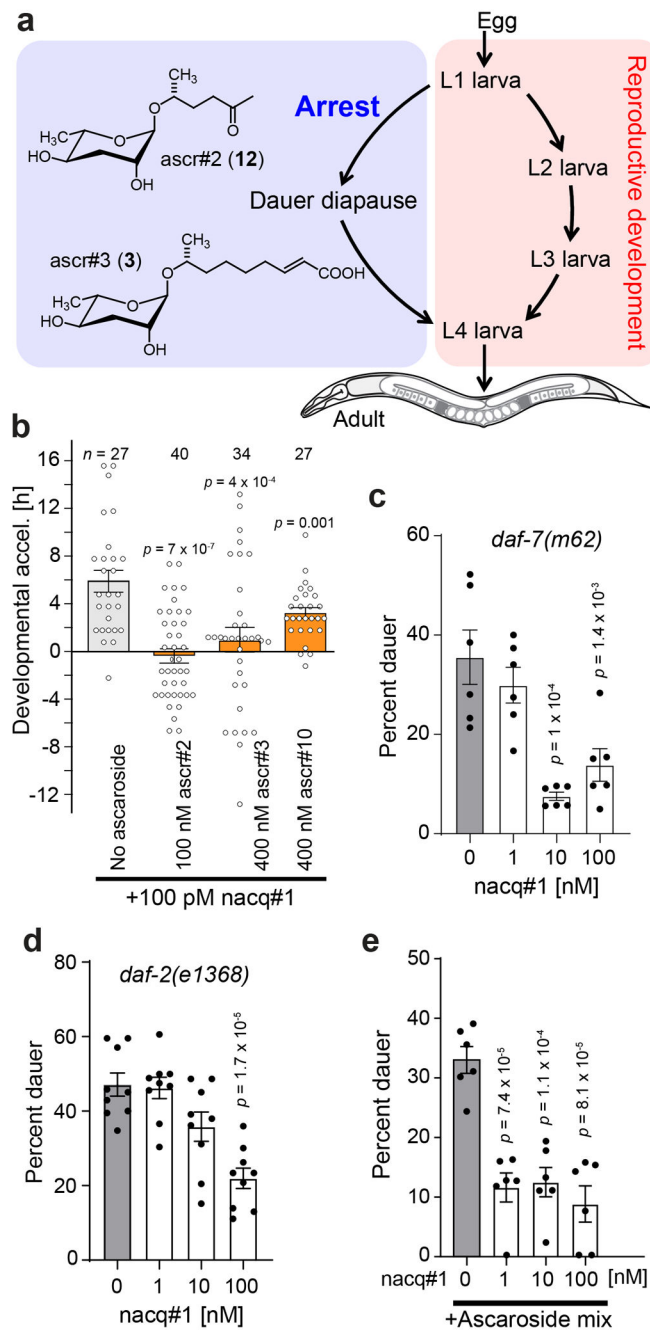


Figure 4 | *nacq#1* and ascarosides are mutually antagonistic signals.

a, Ascarosides, e.g. *ascr#2* and *ascr#3*, induce dauer diapause, a stress-resistant alternate larval stage. **b**, Ascarosides counteract developmental acceleration of *daf-22* mutants treated with *nacq#1* (numbers of worms tested for each condition are indicated in the Figure). For data, see Supplementary Table 11. **c,d**, *nacq#1* promotes exit from the dauer stage in *daf-7* (**c**) and *daf-2* (**d**) mutants ($n = 6$ (*daf-7*) and $n = 9$ (*daf-2*) biologically independent samples). **e**, *nacq#1* counteracts the effects of ascarosides in dauer exit ($n = 6$ biologically independent samples). For dauer data, see Supplementary Table 12. Error bars represent mean \pm s.e.m. and statistics were performed using two-tailed *t*-tests.

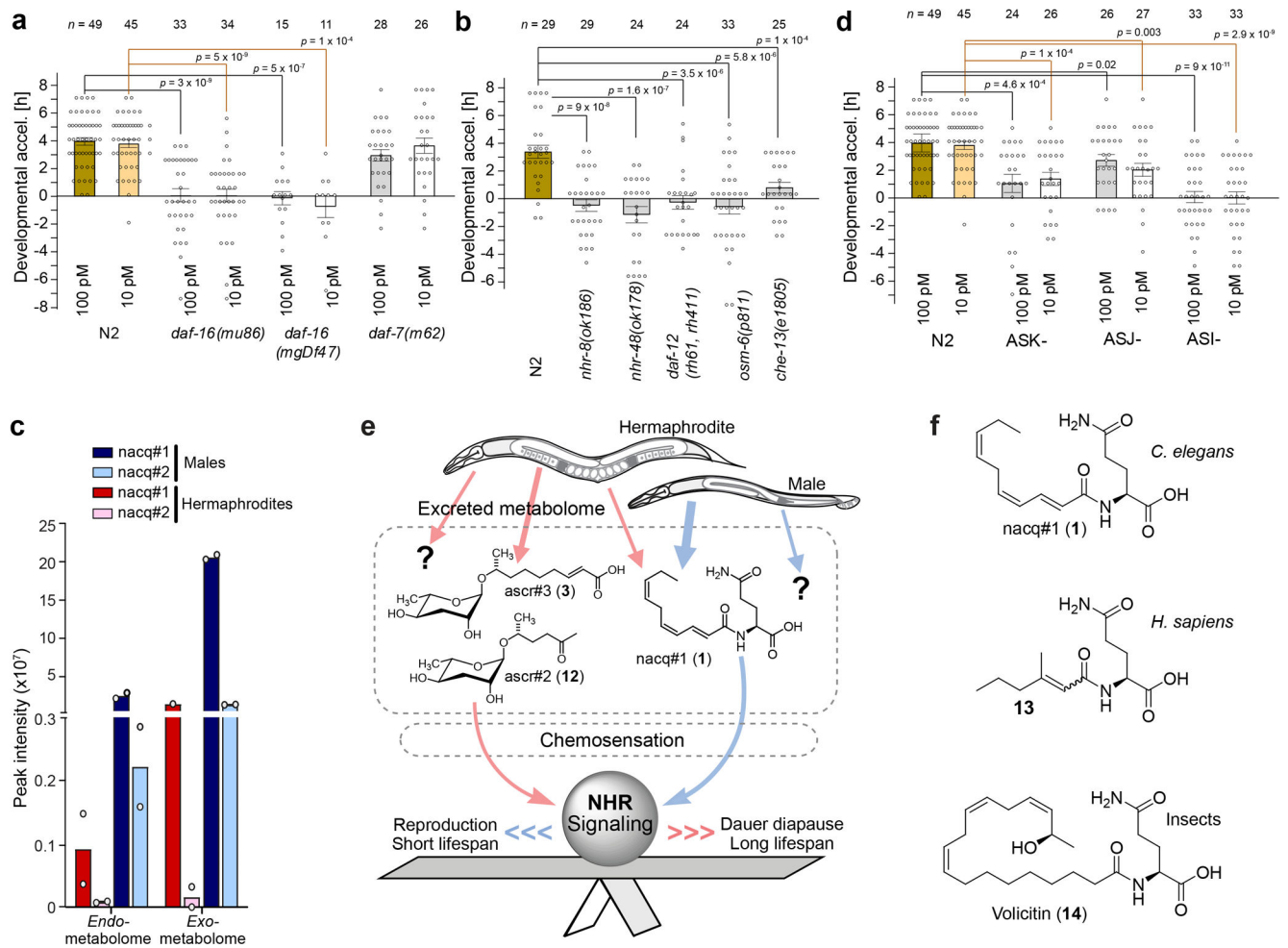


Figure 5 | *nacq#1* signals via conserved signaling pathways.

a, Acceleration of development by the indicated concentrations of *nacq#1* in wild type, *daf-16* and *daf-7* mutants (numbers of worms tested for each condition are indicated in the Figure). **b**, Acceleration of development by *nacq#1* (100 pM) in wild type, *nhr-8*, *nhr-48*, *daf-12*, *osm-6*, and *che-13* mutants (numbers of worms tested for each condition are indicated in the Figure). **c**, HPLC-MS-based quantification of *nacq#1* in the *exo*- and *endo*-metabolomes of *C. briggsae*, collected after the worms reached the young adult stage ($n = 2$ biologically independent samples). **d**, Acceleration of development indicated concentrations of *nacq#1* in wild type (N2) and genetic ablations of the ASI, ASK, or ASJ chemosensory neurons (numbers of worms tested for each condition are indicated in the Figure). **e**, Competing small molecule signals regulate development via NHR signaling. **f**, Chemical structures of *N*-acyl amino acids similar to *nacq#1* identified from other phyla. See Supplementary Tables 13-15 for data in **a**, **b**, and **d**. Error bars represent mean \pm s.e.m. and statistics were performed using two-tailed *t*-tests.